ISSN: 1410-8917
e-ISSN: 2597-9914

Jurnal Kimia Sains dan Aplikasi 23 (6) (2020): 228–233

Jurnal Kimia Sains dan Aplikasi
Journal of Scientific and Applied Chemistry

Journal homepage: http://ejournal.undip.ac.id/index.php/ksa

Synthesis and Characterization of Pyrazine Derived Compounds as Potential Materials for Hole Transporting Layer (HTL)

Vety Sri Harlinda Ayudha [a,*], Mokhamat Ariefin [a]

[a] National Central University, Zhongli, Taoyuan, Taiwan

* Corresponding author: vetyayudha@gmail.com

https://doi.org/10.14710/jksa.23.6.228-233

Article Info

Article history:

Received: 27th December 2019
Revised: 13th May 2020
Accepted: 19th May 2020
Online: 30th June 2020

Keywords:
pyrazine; hole transporting layer (HTL); energy gap

Abstract

Three simple compounds that have the potential as a hole transporting layer (HTL) based on pyrazine derivatives conjugated with electron donor groups in the form of triphenylamine have been successfully synthesized and characterized. The synthesis began with a substitution reaction at high temperatures between 4-bromoaniline and 4-iodoanisole to produce 4-bromo-*N*,*N*-bis(methoxyphenyl)-aniline, followed by substitution of bromo atoms with tributylstanum at low temperatures and inert atmosphere (N_2) producing 4-methoxy-*N*-(4-(tributylstanyl)phenyl)aniline. The conjugation reaction was carried out through a Stille coupling reaction between 1,2-bis (4-bromophenyl)ethane-1,2-dione with 4-methoxy-*N*-(4-(tributylstanyl)phenyl) aniline at high temperatures with the aid of a $Pd(PPh_3)_4$ catalyst in an inert atmosphere (N_2). The reaction was continued with the imination reaction with 3 compounds, i.e., 1,2-diaminobenzene, 3,3-diaminobenzidine and 2,3-diaminopiridin to produce three HTL compounds that were namely 4',4"-(quinoxaline-2,3-diyl)bis (N,N-bis(4(methoxyphenyl)-[1,1'-biphenyl]-4-amine) **(DNB)**, 4',4''',4''''',4'''''''-([6,6'-biquinoxaline]-2,2',3,3'-tetrayl) tetrakis(N,N-bis(4-methoxyphenyl)-[1,1'-biphenyl]-4-amine) **(bDNB)**, and 4',4'''-(pyrido[2,3-b]pyrazine-2,3-diyl)bis(N,N-bis (4-methoxyphenyl)-[1,1'-biphenyl]-4-amine) (**DNP**). The optical and electrochemical properties of **DNB**, **bDNB**, and **DNP** were analyzed by UV-Vis and Differential Pulse Voltammetry (DPV). The optical and electrochemical properties show the energy levels of the HOMO and LUMO of the three compounds. Hence their potential can be estimated as HTL compounds. The three compounds show λ_{max} of 348 nm, 356 nm, and 350 nm for **DNB**, **bDNB**, and **DNP**. Based on DPV results, the HOMO values for **DNB**, **bDNB**, and **DNP** are -5.03 eV, -5.02 eV, and -4.98 eV and LUMO values of -2.46 eV, -2.76 eV and -2.87 eV, respectively. The three compounds' thermal properties were analyzed using TGA, with the results showing that the three compounds had good thermal resistance with a decomposition point above 400°C. Based on optical, electrochemical, and thermal analysis, **DNB** and **bDNB** have almost the same properties. Thus, it is expected that the three compounds have the potential as HTL material, with **DNB** and **bDNB** better than **DNP**.

1. Introduction

The development of electronic technology has been developing quickly; this is followed by the increasing need for electricity usage. Coal is still the primary energy source used in electricity generation. However, the use of coal causes many losses, such as environmental pollution, air pollution [1], or even respiratory disorders [2].

Based on these problems, we need a renewable electricity source that is more environmentally friendly such as hydroelectric energy [3], geothermal electric energy [4], or solar electric energy (solar panels). From several renewable energy sources, solar panels are promising renewable sources because of their unlimited sources. However, the use of solar panels as an energy source still has its challenges in its application, such as

expensive materials or low energy conversion. Based on data compiled by the National Renewable Energy Laboratory (NREL), solar panels made from Si-active crystals still hold the highest conversion efficiency, compared to solar panels with other active ingredients, such as organic solar panels, or perovskite. To that end, researchers in the field of materials to date have tried to find ways to optimize the value of power conversion energy (PCE) from solar panels, both research in the manufacture of devices (devices) or the synthesis of potential compounds for solar panels [5].

Several solar panels have evolved, such as organic photovoltaic (OPV) with active ingredients in the form of small organic compounds or polymers, Si-crystalline, and Perovskite Solar Cells (PSC). Perovskite is a calcium titanium oxide ($CaTiO_3$) mineral that was discovered by Gustave Rose in 1839. In perovskite solar panels, the term perovskite used does not refer to $CaTiO_3$ crystals, but crystalline compounds that have the same structure as $CaTiO_3$ [6]. During its development, one of the perovskites used in solar cells was methylammonium lead halide ($CH_3NH_3PbI(I_3)$) developed by Miyasaka. $CH_3NH_3PbI(I_3)$ as an active component in solar cells has advantages such as low exciton binding energy, sharp optical absorption, and good carrier diffusion-length [7].

PSC is composed of several essential parts, such as transparent conductive layers (IOP, indium tin oxide), the electron transporting layer (ETL), active layer (perovskite), the hole transporting layer (HTL), and metal electrodes. The composition of the PSC can be seen in Figure 1(i). HTL is a part that functions to transfer holes (positive charges) to the electrodes. Generally, this section uses Spiro-OMeTAD (Figure 1 (ii)) as its forming material. However, Spiro-OMeTAD is a compound that is difficult to synthesize and purify, so we need a new compound that is easier to make and has a high PCE when used in PSC [8].

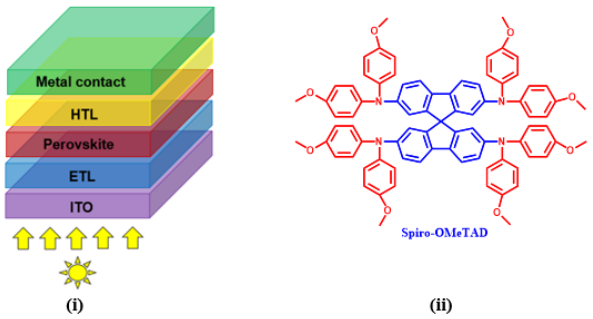

Figure 1. (i) PSC composition; (ii) Spiro-OMeTAD structure

Liu *et al.* [9] succeeded in making a simple HTL based on carbazole derivatives with three electron-rich groups in the form of triphenylamine, named **LD22** with λ_{max} of 381 nm. **LD22** has HOMO and LUMO of -5.27 eV and -2.30 eV, respectively, while Spiro-OMeTAD (λ_{max} = 386 nm) with the same measurement method, has HOMO and LUMO values of -5.14 eV and -2.15 eV. **LD22** achieved PCE up to 13% when applied to the PSC, while Spiro-OmeTAD produced PCE 17.18% when applied to the same device. Cui *et al.* [10] could also synthesize simple HTL compounds from hexaphenylbenzene (**HPB**) derivatives with the donor group triphenylamine. **HPB** has HOMO and LUMO values of -5.20 eV and -2.10 eV with λ_{max} of 367 nm and can reach PCE up to 12.9%. Based on this, then, in this study, developed an organic material based on pyrazine derivatives with an electron donor group triphenylamine, which can be used as HTL.

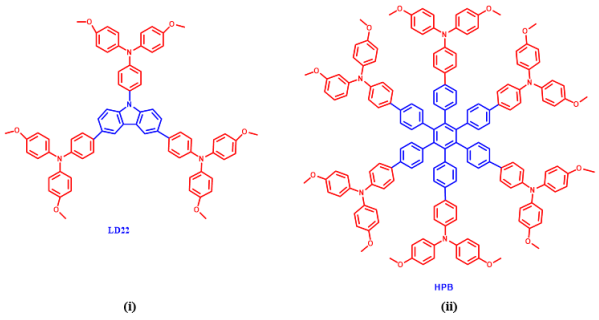

Figure 2. (i) **LD22** structure; (ii) **HPB** structure

2. Methodology

The synthesis of 4',4''-(kuinoksalin-2,3-diil)bis(N,N-bis(4(metoksifenil)-[1,1'-bifenil]-4-amine) **(DNB)**, 4',4''',4''''',4'''''''-([6,6'-biquinoxaline]-2,2',3,3'-tetrayl) tetrakis(N,N-bis(4-methoxyphenyl)-[1,1'-biphenyl]-4-amine) **(bDNB)**, and 4',4'''-(pyridine[2,3-b]pyrazine-2,3-diyl)bis(N,N-bis(4-methoxyphenyl)-[1,1'-biphenyl]-4-amine) **(DNP)** started from synthesis 4-bromo-N,N-bis(4-methoxyphenyl)aniline **(a)** using starting material 4-bromoanilin **(i)** and 4-iodoanisole **(j)** (step **i**). In stage **ii**, the transformation of Br group to tributyltin chloride was carried out through a substitution reaction between compound **(a)** and tributyltin chloride **(d)** to produce 4-methoxy-N-(4-(tributylstanyl)phenyl)aniline **(b)**. Furthermore, the Stille coupling reaction (step **iii**) was carried out between compound **(b)** and 1,2-bis(4-bromophenyl)ethane-1,2-dione **(e)** so that the compound 1,2-bis(4'-bis(4-methoxyphenyl)amino)-[1.1'-biphenyl]-4-il)ethane-1,2-dion **(c)** was obtained. From these compounds, an imitation was carried out using 1,2-diaminobenzidine **(f)**, 2,3-diaminopiridin **(g)**, and 3,3'-diaminobenzidine **(h)** to obtain the desired HTL. The complete scheme can be seen in Figure 3.

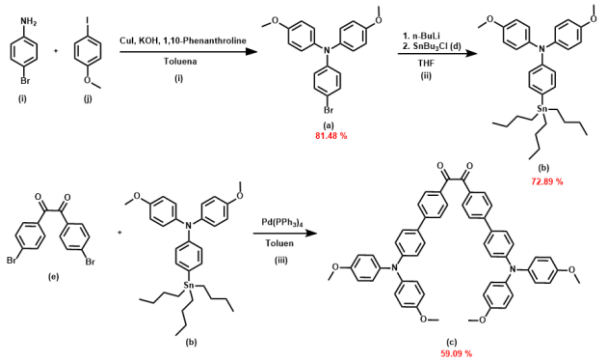

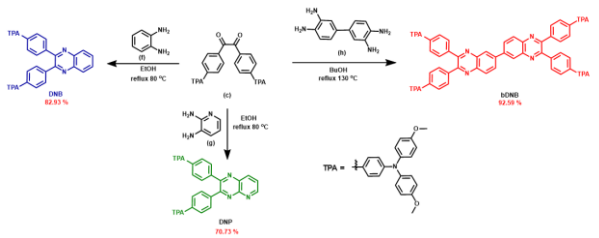

Figure 3. Synthesis of **DNB**, **bDNB**, and **DNP**

2.1. Equipment and Materials

The materials used in the experiment included 4-bromoaniline, 1-iodo-4-methoxybenzene, dry toluene, 2.5 M *n*-butyl lithium, tributyltin chloride, dry tetrahydrofuran (THF), 4,4'-dibromobenzil, tetrakis (triphenylphosphine) palladium ($Pd(PPh_3)4$), 1,2-diaminobenzidine, 2,3-diaminopiridin, 3,3'-diaminobenzidine, ethanol, n-butanol, chloroform-d, ethyl acetate, dichloromethane (DCM), and *n*-hexane. For compound characterization, ^{1}H-NMR and ^{13}C-NMR Bruker Model 300Hz and 500 Hz, Hitachi UV-Vis spectrophotometer, Differential pulse voltammetry (DPV) with Pt and Ag/AgCl electrodes, and Perkin Elmer TGA-7 were used

2.2. Synthesis of 4-bromo-N,N-bis(4-methoxyphenyl)aniline (a)

4-bromoaniline (10 g, 58.13 mmol), 1-iodo-4-methoxybenzene (35.52 g, 14.53 mmol), CuI (0.554 g, 2.91 mmol), KOH (25.44 g, 45.34 mmol), 1,10-phenanthroline (0.419 g, 2.33 mmol) were put into 250 mL of a round bottom flask which has been conditioned on N_2 atmosphere. Then in the mixture, 60 mL of dried toluene was added. The mixture was stirred and refluxed for 24 hours at 120°C. After that, some methanol was added to the mixture, and all the solvents were evaporated. The result of the evaporation was extracted using dichloromethane (DCM) and water. The product was purified using column chromatography with hexane: ethyl acetate (49: 1) eluent to obtain compound **a** (16.5 g, 81.84%) as a white solid. ^{1}H NMR (500 MHz, $CDCl_3$): δ 7.232 ppm (d, 2H, J = 8.50), δ 7.023 ppm (d, 4H, J = 9.00), δ 6.820 ppm (d, 4H, J = 9.00), δ 6.787 ppm (d, 2H, J = 8.50), δ 3.790 ppm (s, 6H).

2.3. Synthesis of 4-methoxy-N-(4-methoxyphenyl)-N-(4- (tributylstanil)phenyl)aniline (b)

Compound **a** (2.01 g, 5.78 mmol) was put into a 100 mL round bottom flask conditioned in N_2 atmosphere, then dissolved using 40 mL dry THF. After that, 2.5 M *n*-butyllithium (2.5 mL, 6.36 mmol) was added to the solution of the compound **a** slowly, at -78°C and stirred for 2 hours (maintaining temperature). After 2 hours, Bu_3SnCl (1.74 mL, 6.35 mmol) was added at -78°C, and the temperature was allowed to rise slowly until it reached room temperature and left overnight. After overnight, the NaCl solution was added to the mixture and extracted using diethyl ether/water. The organic layer obtained was dried using anhydrous sodium sulfate and evaporated. The crude was purified by distillation to obtain compound **b** (2.5 g, yield 72.89%) as a yellow liquid. ^{1}H NMR (500 MHz, $CDCl_3$): δ 7.229 ppm (d, 2H, J = 8.00), δ 7.057 ppm (d, 4H, J = 8.50), δ 6.886 ppm (d, 2H, J = 8.00), δ 6.817 ppm (d, 4H, J = 9.00), δ 3.789 ppm (s, 6H).

2.4. Synthesis of 1,2-bis(4'-bis(4-methoxyphenyl)amino)-[1,1'-biphenyl]-4-il)ethane-1,2-dion (c)

Compounds **b** (1.29 g, 2.17 mmol), $Pd(PPh_3)4$ (63 mg, 0.055 mmol), and 1,2-bis(4-bromophenyl)ethane-1,2-dione (200 mg, 0.54 mmol) were put into a 100 mL round bottom flask which had been conditioned in N_2 atmosphere. Then, it was dissolved using 30 mL dry toluene. The solution was refluxed for 48 hours. After that, the reaction mixture was filtered using celite and washed with ethyl acetate. Then, all the solvents were evaporated. The evaporation results were purified using column chromatography with eluents of hexane: ethyl acetate (4: 1) to obtain compound **c** (260 mg, 59.09% yield) as an orange solid. ^{1}H NMR (500 MHz, $CDCl_3$): δ 8.009 ppm (d, 2H, J = 8.50), δ 7.672 ppm (d, 2H, J = 8.50), δ 7.452 ppm (d, 2H, J = 9.00), δ 7.101 ppm (d, 4H, J = 8.50), δ 6.968 (d, 2H, J = 8.50), δ 6.857 ppm (d, 4H, J = 8.50), δ 3.806 ppm (s, 6H).

2.5. Synthesis of DNB

Compounds **c** (75 mg, 0.09 mmol) and 1,2-diaminobenzene (11 mg, 0.101 mmol) were mixed into a 100 mL round bottom flask and dissolved in 30 mL ethanol. The mixture was refluxed for 24 hours. After that, the reaction mixture was filtered and the solids were washed using ethanol, so that a **DNB** (68 mg, 82.93% yield) was obtained as a yellow solids ^{1}H NMR (500 MHz, $CDCl_3$): δ 8.177 ppm (dd, 2H, J = 6.00), δ 7.766 ppm (dd, 2H, J = 6.00), δ 7.613 ppm (d, 4H, J = 8.50), δ 7.545 ppm (d, 4H, J = 8.00), δ 7.444 (d, 4H, J = 8.50), δ 7.083 (d, 8H, J = 8.50), δ 6.980 (d, 4H, J = 8.50), δ 6.842 ppm (d, 8H, J = 8.50), δ 3.804 ppm (s, 12H).

2.6. Synthesis of bDNB

Compounds **c** (55 mg, 0.07 mmol) and 3,3-diaminobenzidine (6.5 mg, 0.03 mmol) were mixed into 100 mL round bottom flask and dissolved in 30 mL butanol. The mixture was refluxed for 24 hours. After that, the reaction mixture was filtered and the solid was washed using ethanol, so **bDNB** (50 mg, 92.59% yield) was obtained in the form of orange solids. ^{1}H NMR (500 MHz, $CDCl_3$): δ 8.593 ppm (s, 2H), δ 8.310 ppm (d, 2H, J = 9.00), δ 8.232 ppm (d, 2H, J = 8.50), δ 7.661 ppm (d, 2H) 8H, J = 7.50), δ 7.572 (d, 8H, J = 7.00), δ 7,462 (d, 8H, J = 8.50), δ 7,091 (d, 16H, J = 8.50), δ 6,991 (d, 8H, J = 9.00), δ 6,848 ppm (d, 16H, J = 9.00), δ 3.808 ppm (s, 24H).

2.7. Synthesis of DNP

Compounds **c** (75 mg, 0.09 mmol) and 2,3-diaminopiridin (11 mg, 0.101 mmol) were mixed into 100 mL round bottom flask and dissolved in 30 mL ethanol. The mixture was refluxed for 24 hours. After that, the reaction mixture was filtered, and the solid was washed using methanol. Then the crude was purified by column chromatography with hexane: ethyl acetate (2: 1) eluent

to obtain **DNP** (58 mg, 70.73% yield) in the form of orange solids. ^{1}H NMR (500 MHz, $CDCl_3$): δ 9.156 ppm (s, 1H), δ 8.518 ppm (d, 1H, J = 7.00), δ 7.733 ppm (m, 3H), δ 7.643 ppm (m, 2H), δ 7.570 (d, 4H, J = 9.00), δ 7.457 ppm (b, 4H), δ 7.077 ppm (b, 8H), δ 6.842 ppm (d, 4H, J = 8.50), δ 6.845 ppm (d, 8H, J = 8.00), δ 3.804 ppm (s, 12H).

2.8. NMR analysis

NMR is a qualitative analysis method for determining the chemical structure of a compound. In this study, ^{1}H-NMR was used, spectra were recorded with 300 MHz Bruker and 500 MHz using $CDCl_3$ solvent.

2.9. Ultraviolet-visible (UV-Vis) analysis

All final compounds were analyzed using a UV-Vis spectrophotometer. *O*-dichlorobenzene was used as a solvent and a blank solution. The cuvette used was made of orz with a thickness of 10 mm. The results of the UV analysis were used to calculate the energy gap (Eg) with the formula:

$$E_g = \frac{1243}{\lambda_{onset}}\ eV$$

2.10. Differential Pulse Voltammetry (DPV) Analysis

Differential Pulse Voltammetry (DPV) analysis is used to determine the HOMO-LUMO level of the final compound. *O*-dichlorobenzene was used as a solvent. DPV was measured in an inert condition (N_2) and was used ferrocene as an internal standard in measurement.

3. Results and Discussion

3.1. Optical properties

The results of the UV-Vis analysis of **DNB**, **bDNB**, and **DNP** compounds are presented in Figure 4. Based on these spectra results, the values of λ_{max} for **DNB**, **bDNB**, and **DNP** are 348.5 nm, 356 nm, and 350 nm. In the **bDNB** compound, the absorption peak produced was not significantly different even though it was more conjugated than the other two compounds. This can be explained because, in **bDNB** compounds, the bond between C atoms in one benzene ring and C in another benzene rotates (there is a dihedral angle), so the conjugation of **bDNB** becomes imperfect [11]. This gives an effect on the value of λ_{max} obtained. Based on these data, the three compounds have λ_{max} below 400 nm, as well as the Spiro-OMeTAD uptake (λ_{max} = 386 nm) [9], so that the absorption does not overlap with the absorption of perovskite. The existence of additional peaks that overlap with the perovskite absorption often leads to reduced photocurrent in the solar panel, thus disrupting the efficiency of the solar panel [12].

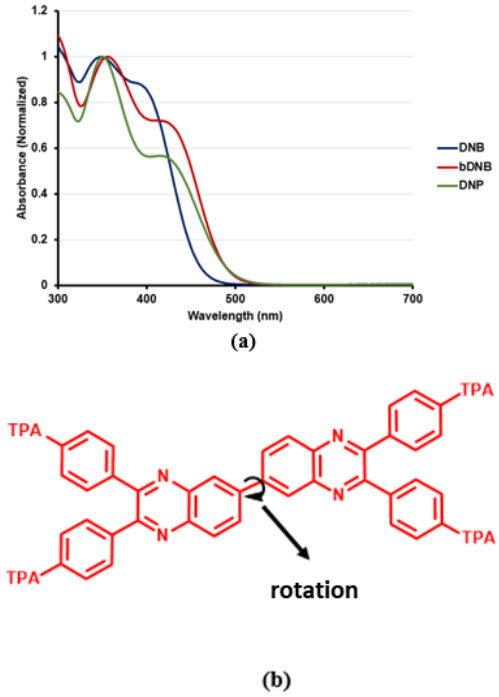

Figure 4. (a) UV-Vis spectra of **DNB**, **bDNB**, and **DNP**; (b) Rotation on **bDNB**

The energy gap (E_g) values of **DNB**, **bDNB**, and **DNP** from optical calculations are 2.65 eV, 2.5 eV, and 2.49 eV. E_g of **DNB** is higher when compared to **DNP** because N atom is more electronegative than C atom (on the benzene **DNB** ring), so N atom can decrease the LUMO level of **DNP**. The optical properties of the three compounds are summarized in Table 1.

Table 1. Optical properties of **DNB**, **bDNB**, and **DNP**

Compound	λ_{max} (nm)	λ_{onset} (nm)	E_{gap} (eV)
DNB	348	467	2.65
bDNB	356	496.5	2.50
DNP	350	497.5	2.49

3.2. Electrochemical properties

DPV analysis is used to obtain the reduction potential and oxidation potential of **DNB**, **bDNB**, and **DNP**, so the HOMO-LUMO value of each compound can be calculated. The values of HOMO, LUMO, reduction potential, oxidation potential, and E_g of the three compounds are summarized in Table 2. The LUMO values for the three compounds are -2.46 eV, -2.76 eV, and -2.87 eV for **DNB**, **bDNB**, and **DNP**. In **DNB** and **bDNB** compounds, different LUMO values are obtained, because **bDNB** has more electron-pushing groups than **DNB**, so the LUMO level of **bDNB** is more negative. The LUMO value on **DNP** is more negative when compared to the analogs, namely **DNB**. This more negative value is due to the presence of more electronegative N atoms in the pyridine ring. In contrast to LUMO, the HOMO values in the three compounds do not differ significantly. The overall energy level of HOMO-LUMO in the three compounds is illustrated using the diagram in Figure 5.

Spiro-OMeTAD is a commercial compound used as HTL material in general, having HOMO, LUMO, and Eg

values of -5.14 eV, -2.15 eV, and 2.99 eV, respectively [9]. For PSC applications, the HOMO value must be more positive than the HOMO value of perovskite (HOMO value $CH_3NH_3PbI_3$ = -5.4 eV) [13], so that the hole more easily flow towards the electrode. In line with HOMO, the LUMO value from HTL must be more positive than the LUMO from perovskite (LUMO value $CH_3NH_3PbI_3$ = -3.9 eV) [13], thus preventing electrons from flowing towards HTL. The three new HTL compounds that have been synthesized, both **DNB**, **bDNB**, and **DNP**, have HOMO-LUMO characteristics that are not much different from Spiro-OMeTAD. Thus, it is expected that the three compounds can be applied as HTL in PSC.

Table 2. Electrochemical properties of **DNB**, **bDNB**, and **DNP**

Compound	E_{re} (V)	E_{ox}(V)	LUMO (eV)	HOMO (eV)	E_{gap} (eV)
DNB	-1.74	0.83	-2.46	-5.03	2.57
bDNB	-1.44	0.82	-2.76	-5.02	2.26
DNP	-1.33	0.78	-2.87	-4.98	2.10

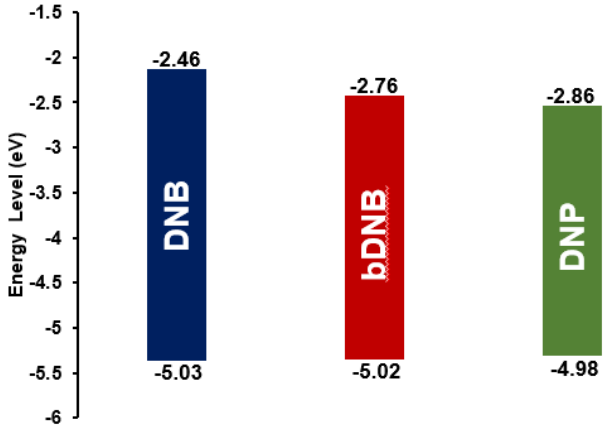

Figure 5. Energy level diagram of **DNB**, **bDNB**, and **DNP**

3.3. Thermal properties

Thermal properties were analyzed using Thermogravimetric analysis (TGA) to determine the heat resistance of the three final compounds synthesized. Besides TGA, the melting point apparatus is also used to determine the melting point of each compound. Based on the melting point apparatus results, the melting points for **DNB**, **bDNB**, and **DNP** were obtained respectively 254.3°C, 290.2°C, and 257.5°C. The melting point of the three compounds is higher than that of Spiro-OMeTAD (commercial HTL), which has a melting point of 240°C. Based on the TGA results, a decomposition point (5% weight loss) from **DNB**, **bDNB**, and **DNP** were obtained at temperatures of 437.3°C, 445.6°C and 400.9°C respectively, while Spiro-OMeTAD was at 424°C [14]. Based on these data, it is obtained that **bDNB** has the highest decomposition point. This is possible because **bDNB** has a higher molecular weight than the other two. From the TGA results, it can be concluded that the three compounds have good thermal stability to be used as HTL material.

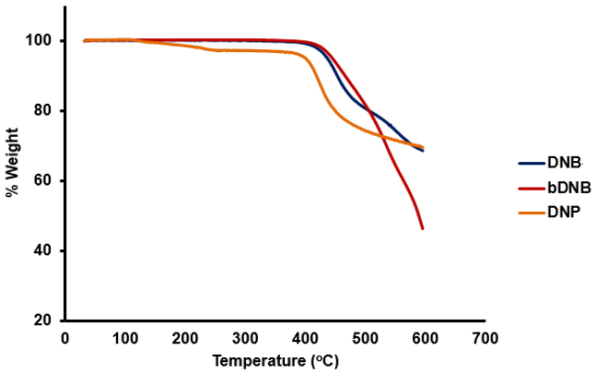

Figure 6. TGA graph of **DNB**, **bDNB**, and **DNP**

4. Conclusions

Three new pyrazine-based compounds, **DNB**, **bDNB**, and **DNP** have been successfully synthesized and characterized. Based on UV-Vis observations, the three compounds had λ_{max}, each of 348.5 nm, 356 nm, and 350 nm for **DNB**, **bDNB**, and **DNP** (while in commercial Spiro-OMeTAD, λ_{max} = 386 nm). Based on DPV results, the HOMO values for **DNB**, **bDNB**, and **DNP** are -5.03 eV, -5.02 eV, and -4.98 eV, while the LUMO values are -2.46 eV, -2.76 eV, and -2.87 eV, respectively. The HOMO-LUMO value of the three compounds is not much different from the HOMO-LUMO from Spiro-OMeTAD (HOMO = -5.14 eV, LUMO = -2.14). The melting points for **DNB**, **bDNB**, and **DNP** are 254.3°C, 290.2°C, and 257.5°C respectively, which is higher than that of Spiro-OMeTAD (240°C), with a decomposition point of 437.3°C, 445.6°C, and 400.9°C. The decomposition point of the three compounds is above 400°C, so it can be said that the three compounds have good thermal stability. With the appropriate optical, electrochemical, and thermal properties (almost the same as the commonly known HTL, Spiro-OMeTAD), it is expected that **DNB**, **bDNB**, and **DNP** have the potential to be applied as HTL on perovskite solar panels, with **DNB** and **bDNB** being better than with **DNP**.

Acknowledgments

We thank to National Central University of Taiwan for laboratory and instruments support.

References

[1] Sribas Goswami, Impact of coal mining on environment, *European Researcher. Series A*, 92, 3, (2015), 185-196 https://doi.org/10.13187/er.2015.92.185

[2] A. Scott Laney, David N. Weissman, Respiratory diseases caused by coal mine dust, *Journal of occupational and environmental medicine/American College of Occupational and Environmental Medicine*, 56, (2014), S18-S22 https://dx.doi.org/10.1097%2FJOM.0000000000000260

[3] Mario T..L. Barros, Frank T. C. Tsai, Shu-li Yang, Joao E. G. Lopes, William W. G. Yeh, Optimization of large-scale hydropower system operations, *Journal of Water Resources Planning and Management*, 129, 3, (2003), 178-188 https://doi.org/10.1061/(ASCE)0733-9496(2003)129:3(178)

[4] Nasruddin, M. Idrus Alhamid, Yunus Daud, Arief Surachman, Agus Sugiyono, H. B. Aditya, T. M. I. Mahlia, Potential of geothermal energy for electricity generation in Indonesia: A review, *Renewable and Sustainable Energy Reviews*, 53, (2016), 733-740 https://doi.org/10.1016/j.rser.2015.09.032

[5] Joel Jean, Patrick R. Brown, Robert L. Jaffe, Tonio Buonassisi, Vladimir Bulović, Pathways for solar photovoltaics, *Energy & Environmental Science*, 8, 4, (2015), 1200-1219 https://doi.org/10.1039/C4EE04073B

[6] Osbel Almora, Lídice Vaillant-Roca, Germà Garcia-Belmonte, Perovskite solar cells: a brief introduction and some remarks, *Revista cubana de fisica*, 34, 1, (2017), 58-68

[7] Akihiro Kojima, Kenjiro Teshima, Yasuo Shirai, Tsutomu Miyasaka, Organometal halide perovskites as visible-light sensitizers for photovoltaic cells, *Journal of the American Chemical Society*, 131, 17, (2009), 6050-6051 https://doi.org/10.1021/ja809598r

[8] Ajay Kumar Jena, Youhei Numata, Masashi Ikegami, Tsutomu Miyasaka, Role of spiro-OMeTAD in performance deterioration of perovskite solar cells at high temperature and reuse of the perovskite films to avoid Pb-waste, *Journal of Materials Chemistry A*, 6, 5, (2018), 2219-2230 https://doi.org/10.1039/C7TA07674F

[9] Xuepeng Liu, Xiaoqiang Shi, Cheng Liu, Yingke Ren, Yunzhao Wu, Weng Yang, Ahmed Alsaedi, Tasawar Hayat, Fantai Kong, Xiaolong Liu, Yong Ding, Jianxi Yao, Songyuan Dai, A Simple Carbazole-Triphenylamine Hole Transport Material for Perovskite Solar Cells, *The Journal of Physical Chemistry C*, 122, 46, (2018), 26337-26343 https://doi.org/10.1021/acs.jpcc.8b08168

[10] Bin-Bin Cui, Ying Han, Ning Yang, Shuangshuang Yang, Liuzhu Zhang, Yue Wang, Yifei Jia, Lin Zhao, Yu-Wu Zhong, Qi Chen, Propeller-Shaped, Triarylamine-Rich, and Dopant-Free Hole-Transporting Materials for Efficient n–i–p Perovskite Solar Cells, *ACS Applied Materials & Interfaces*, 10, 48, (2018), 41592-41598 https://doi.org/10.1021/acsami.8b15423

[11] Young Soo Kwon, Jongchul Lim, Hui-Jun Yun, Yun-Hi Kim, Taiho Park, A diketopyrrolopyrrole-containing hole transporting conjugated polymer for use in efficient stable organic–inorganic hybrid solar cells based on a perovskite, *Energy & Environmental Science*, 7, 4, (2014), 1454-1460 http://dx.doi.org/10.1039/C3EE44174A

[12] Frédéric Leroux, Atropisomerism, Biphenyls, and Fluorine: A Comparison of Rotational Barriers and Twist Angles, *ChemBioChem*, 5, 5, (2004), 644-649 https://doi.org/10.1002/cbic.200300906

[13] Chih-Hsin Chen, Yu-Ting Hsu, Bo-Cheng Wang, Chung-Lin Chung, Chih-Ping Chen, Thienoisoindigo-Based Dopant-Free Hole Transporting Material for Efficient p–i–n Perovskite Solar Cells with the Grain Size in Micrometer Scale, *The Journal of Physical Chemistry C*, 123, 3, (2019), 1602-1609 https://doi.org/10.1021/acs.jpcc.8b10070

[14] Jagadish Salunke, Xing Guo, Zhenhua Lin, João R. Vale, Nuno R. Candeias, Mathias Nyman, Staffan Dahlström, Ronald Österbacka, Arri Priimagi, Jingjing Chang, Paola Vivo, Phenothiazine-Based Hole-Transporting Materials toward Eco-friendly Perovskite Solar Cells, *ACS Applied Energy Materials*, 2, 5, (2019), 3021-3027 https://doi.org/10.1021/acsaem.9b00408

Supporting Information

1. NMR Spectra

1.1. ^{1}H NMR (500 MHz) 4-bromo-N,N-bis(4-methoxyphenyl)aniline (a)

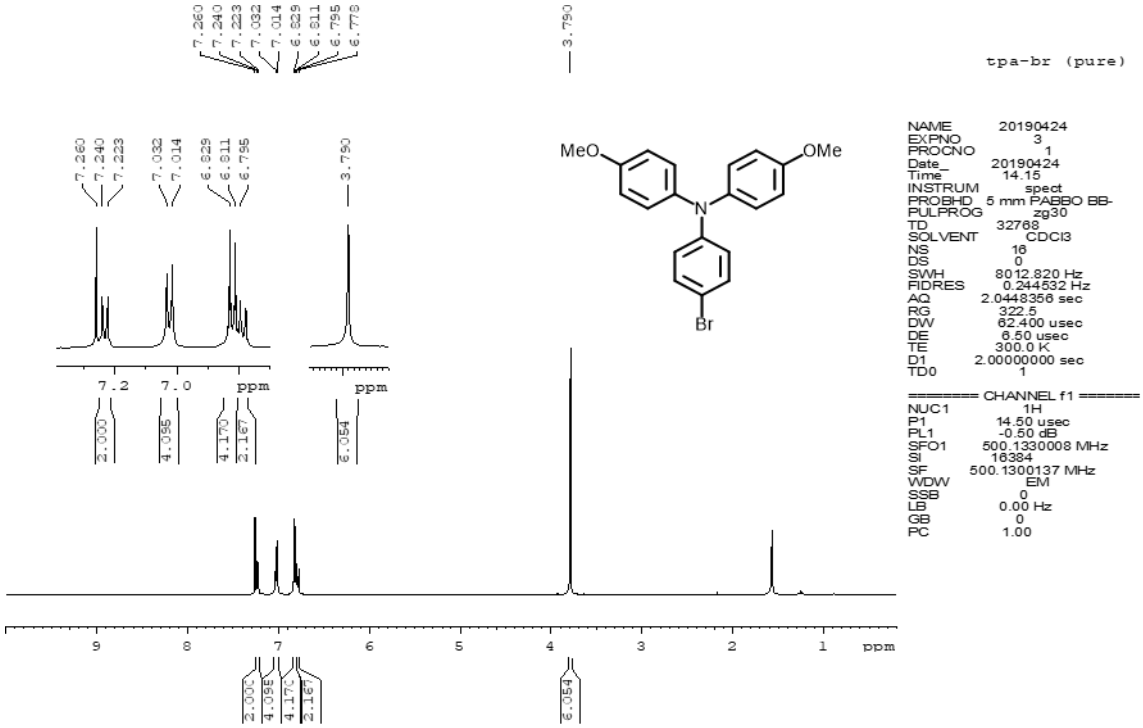

1.2. ^{1}H NMR (500 MHz) 4-metoksi-*N*-(4-metoksifenil)-*N*-(4-(tributilstanil)fenil)anilin (b)

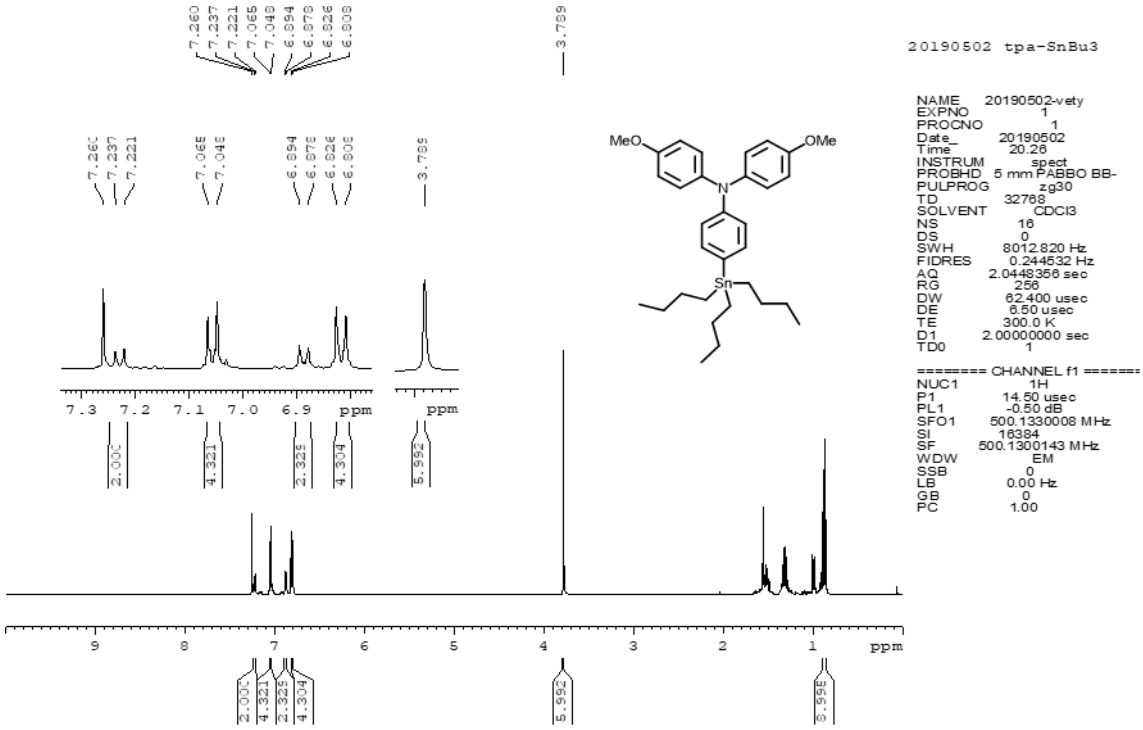

1.3. ^{1}H NMR (500 MHz) 1,2-bis(4'-bis(4-methoxyphenyl)amino)-[1.1'-biphenyl]-4-il)ethane-1,2-dion (c)

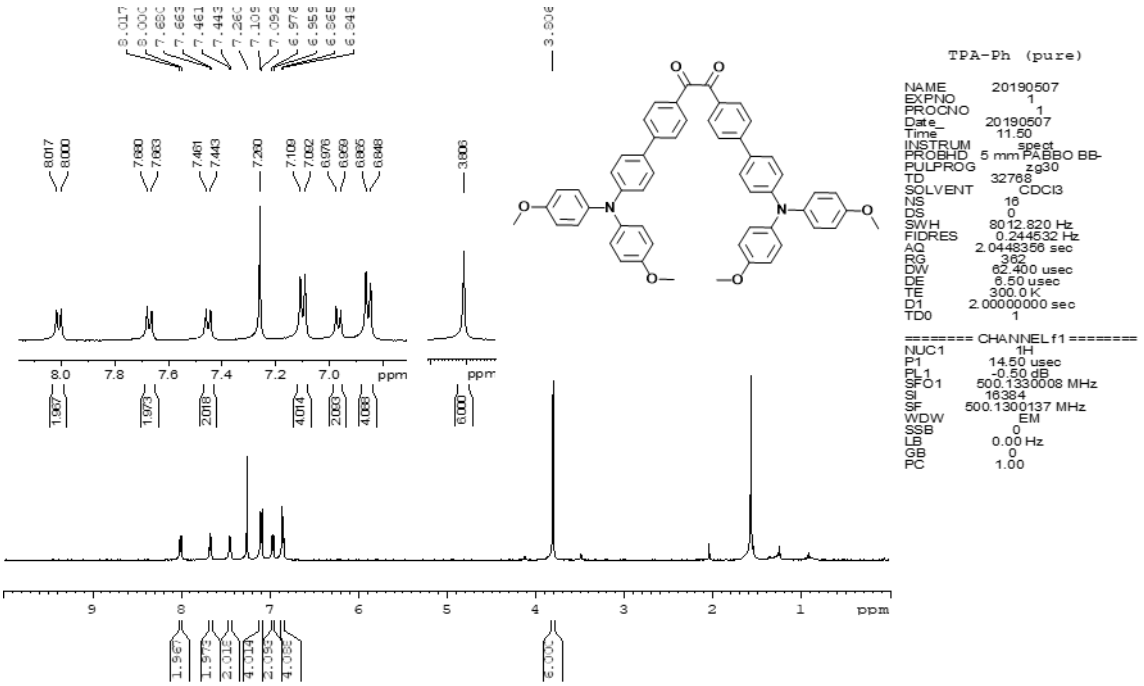

1.4. ^{1}H NMR (500 MHz) DNB

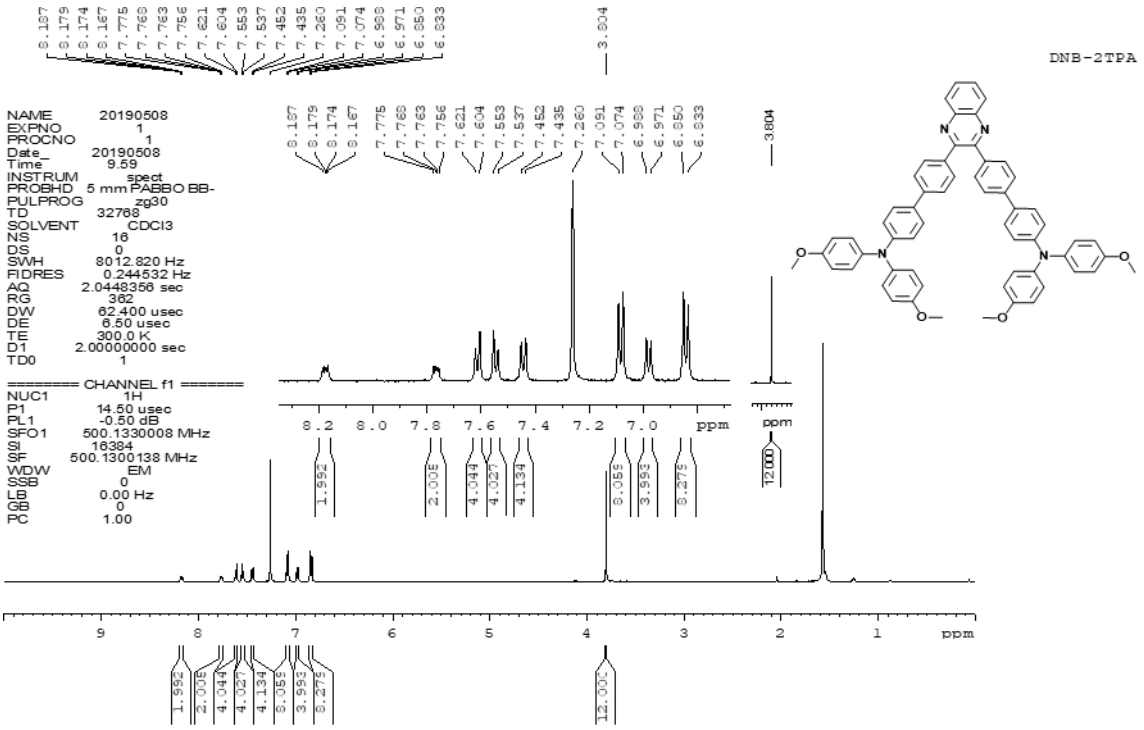

1.5. ^{1}H NMR (500 MHz) DNP

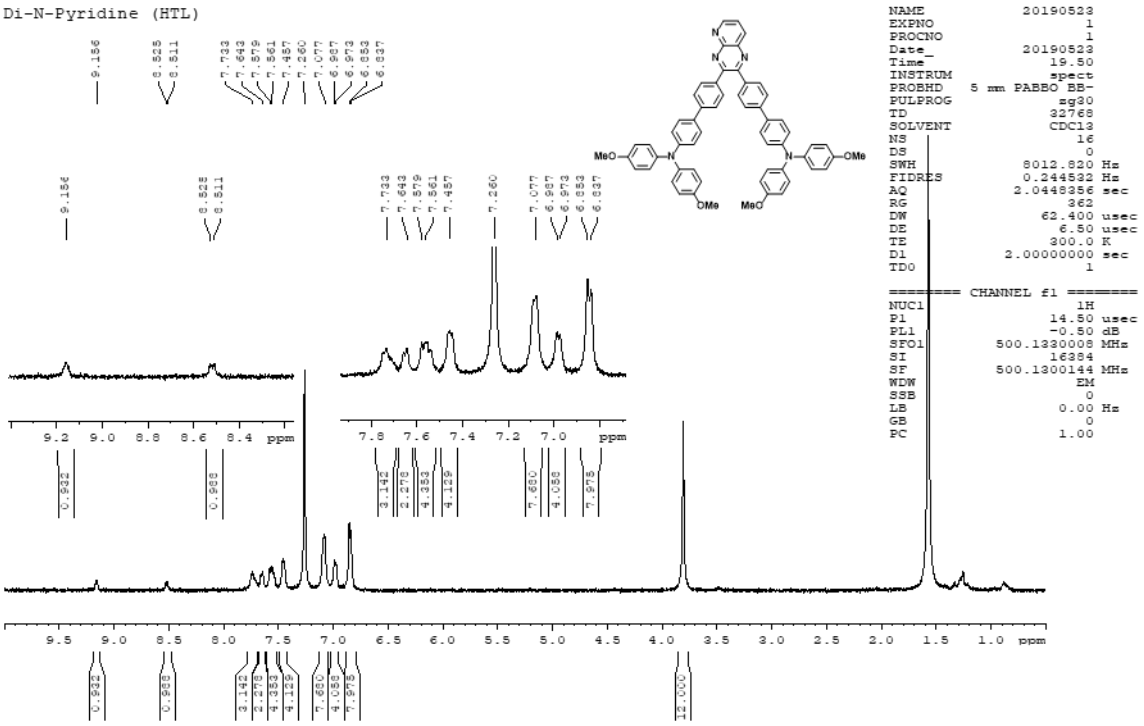

1.6. ^{1}H NMR (500 MHz) bDNB

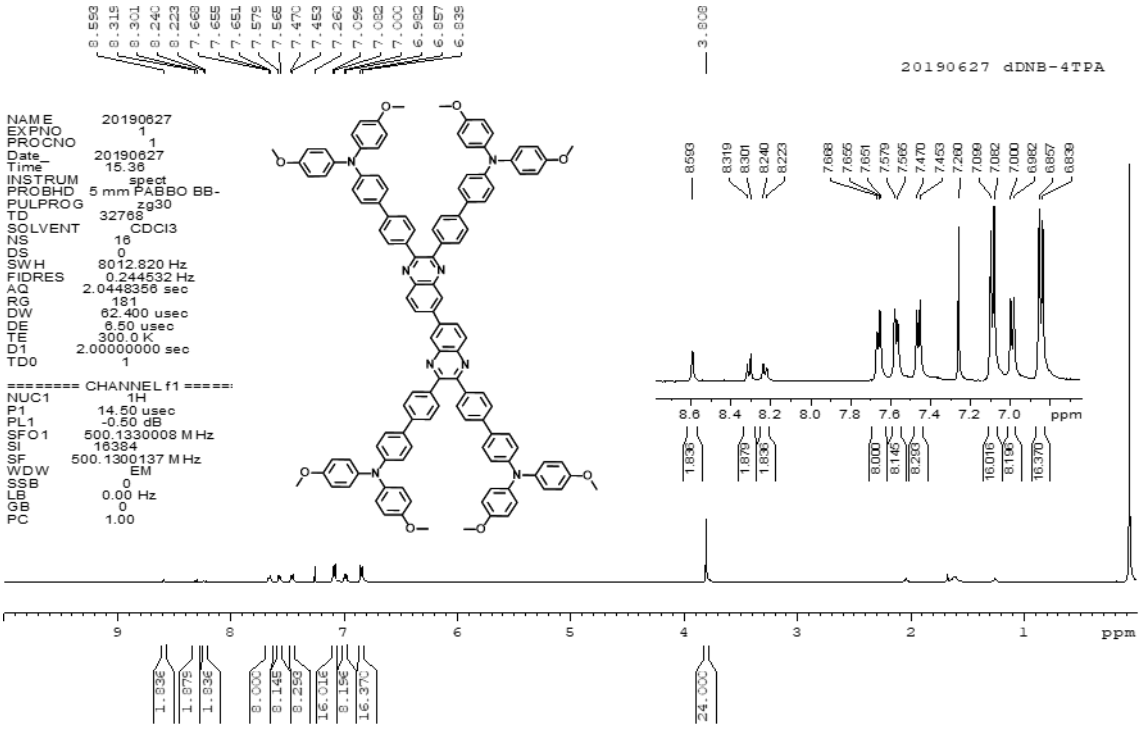

1.7. ^{13}C NMR (500 MHz) DNB

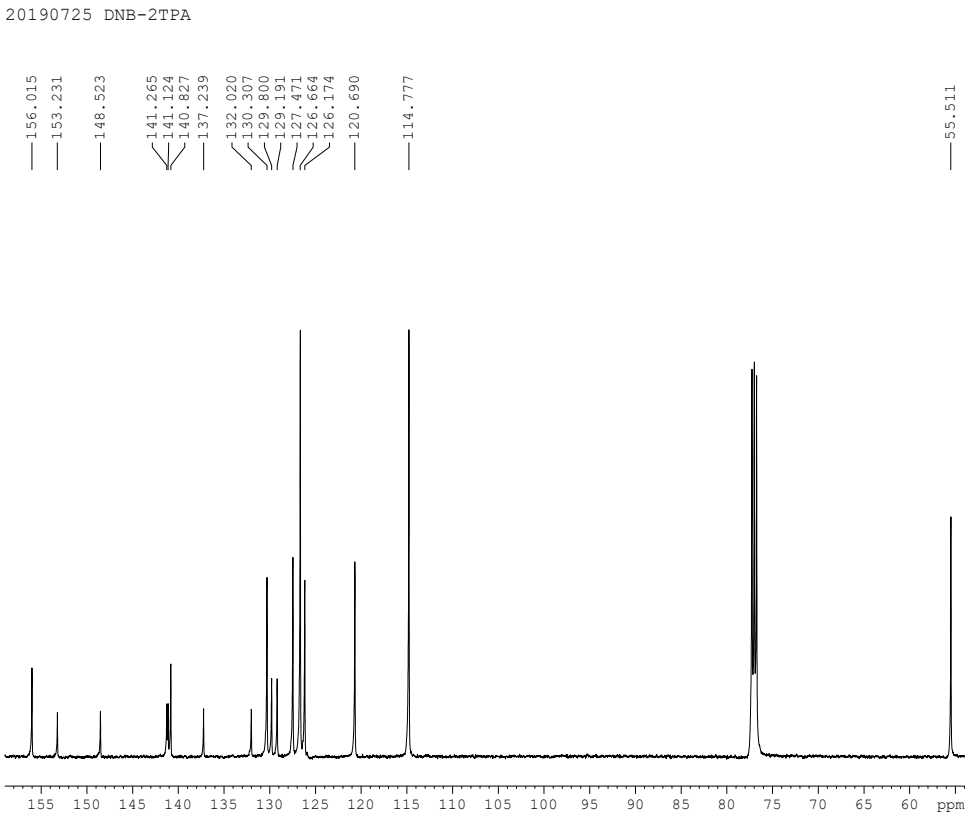


```
NAME            20190725
EXPNO                  2
PROCNO                 1
Date_           20190725
Time                21.02
INSTRUM             spect
PROBHD   5 mm PABBO BB-
PULPROG            zgpg30
TD                  30026
SOLVENT             CDCl3
NS                  36870
DS                      0
SWH            30030.029 Hz
FIDRES          1.000134 Hz
AQ             0.4999996 sec
RG                  26008
DW                16.650 usec
DE                 6.50 usec
TE                300.0 K
D1           0.50000000 sec
D11          0.03000000 sec
TD0                     1

======== CHANNEL f1 ========
NUC1                13C
P1                10.50 usec
PL1                4.20 dB
SFO1        125.7709931 MHz

======== CHANNEL f2 ========
CPDPRG2          waltz16
NUC2                1H
PCPD2             80.00 usec
PL2               -0.50 dB
PL12              13.90 dB
PL13              16.90 dB
SFO2        500.1320005 MHz
SI                  32768
SF          125.7577890 MHz
WDW                    EM
SSB                     0
LB                 3.00 Hz
GB                      0
PC                   1.00
```

1.8. ^{13}C NMR (500 MHz) bDNB

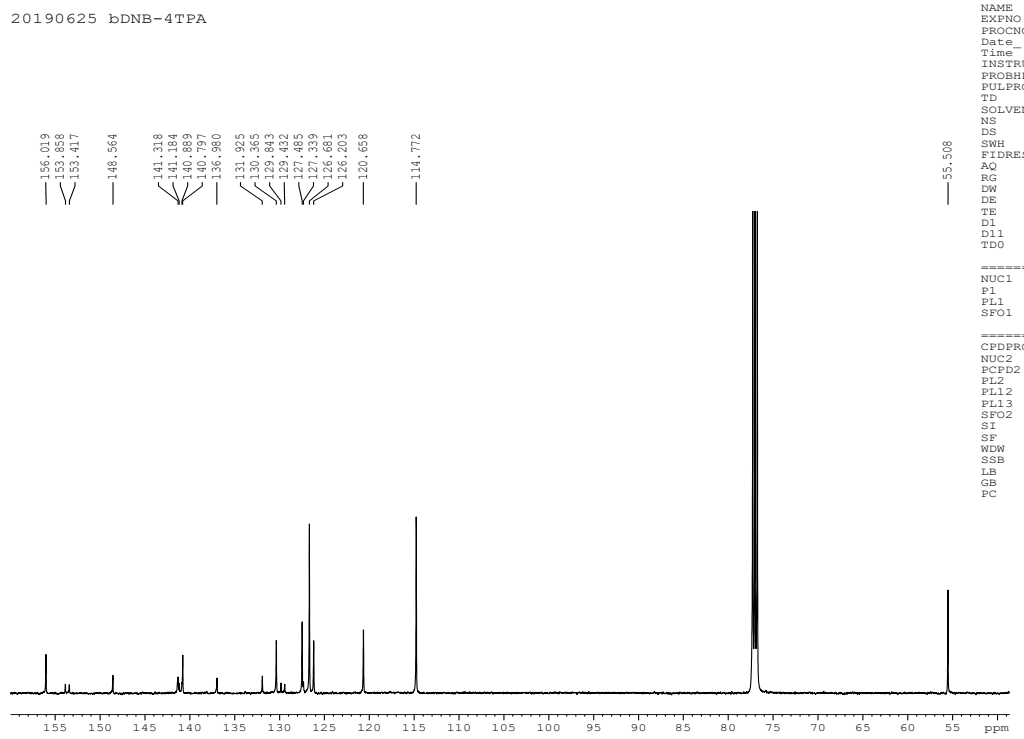


```
NAME            20190625
EXPNO                  1
PROCNO                 1
Date_           20190625
Time                21.25
INSTRUM             spect
PROBHD   5 mm PABBO BB-
PULPROG            zgpg30
TD                  30026
SOLVENT             CDCl3
NS                  35400
DS                      0
SWH            30030.029 Hz
FIDRES          1.000134 Hz
AQ             0.4999996 sec
RG                  23170.5
DW                16.650 usec
DE                 6.50 usec
TE                300.0 K
D1           0.50000000 sec
D11          0.03000000 sec
TD0                     1

======== CHANNEL f1 ========
NUC1                13C
P1                10.50 usec
PL1                4.20 dB
SFO1        125.7709931 MHz

======== CHANNEL f2 ========
CPDPRG2          waltz16
NUC2                1H
PCPD2             80.00 usec
PL2               -0.50 dB
PL12              13.90 dB
PL13              16.90 dB
SFO2        500.1320005 MHz
SI                  32768
SF          125.7577890 MHz
WDW                    EM
SSB                     0
LB                 3.00 Hz
GB                      0
PC                   1.00
```

2. Mass Spectra (MS)

2.1. Mass Spectra of DNB (Exact Mass = 888.3676)

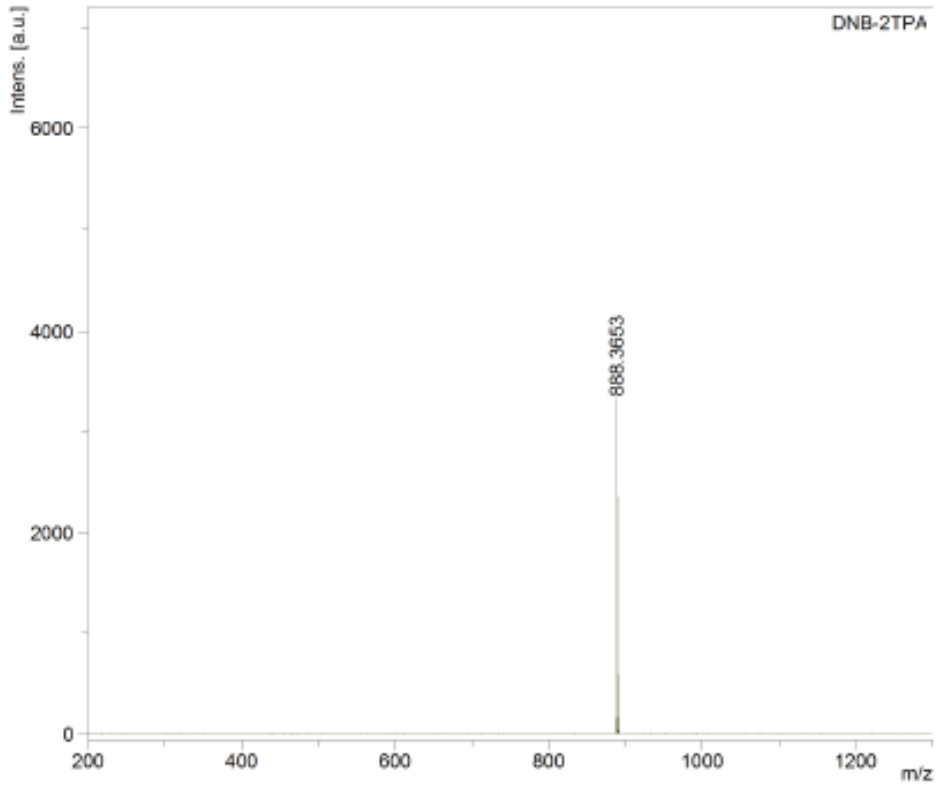

Acquisition Parameter

Date of acquisition	2019-05-30T16:08:00.000
Acquisition method name	D:\Methods\flexControl\Methods\Teresac\RP-PEG 300-1000 -Da 2018-11.par
Aquisition operation mode	Reflector
Voltage polarity	POS
Number of shots	2000
Name of spectrum used for calibration	
Calibration reference list used	PEG-Na -Calibration Mono

Instrument Info

User	NCU
Instrument	ATS-00870
Instrument type	autoflex

Bruker Daltonics flexAnalysis printed: 2019-05-30 4:12:16 PM

2.2. Mass Spectra of DNP (Exact Mass = 889.3628)

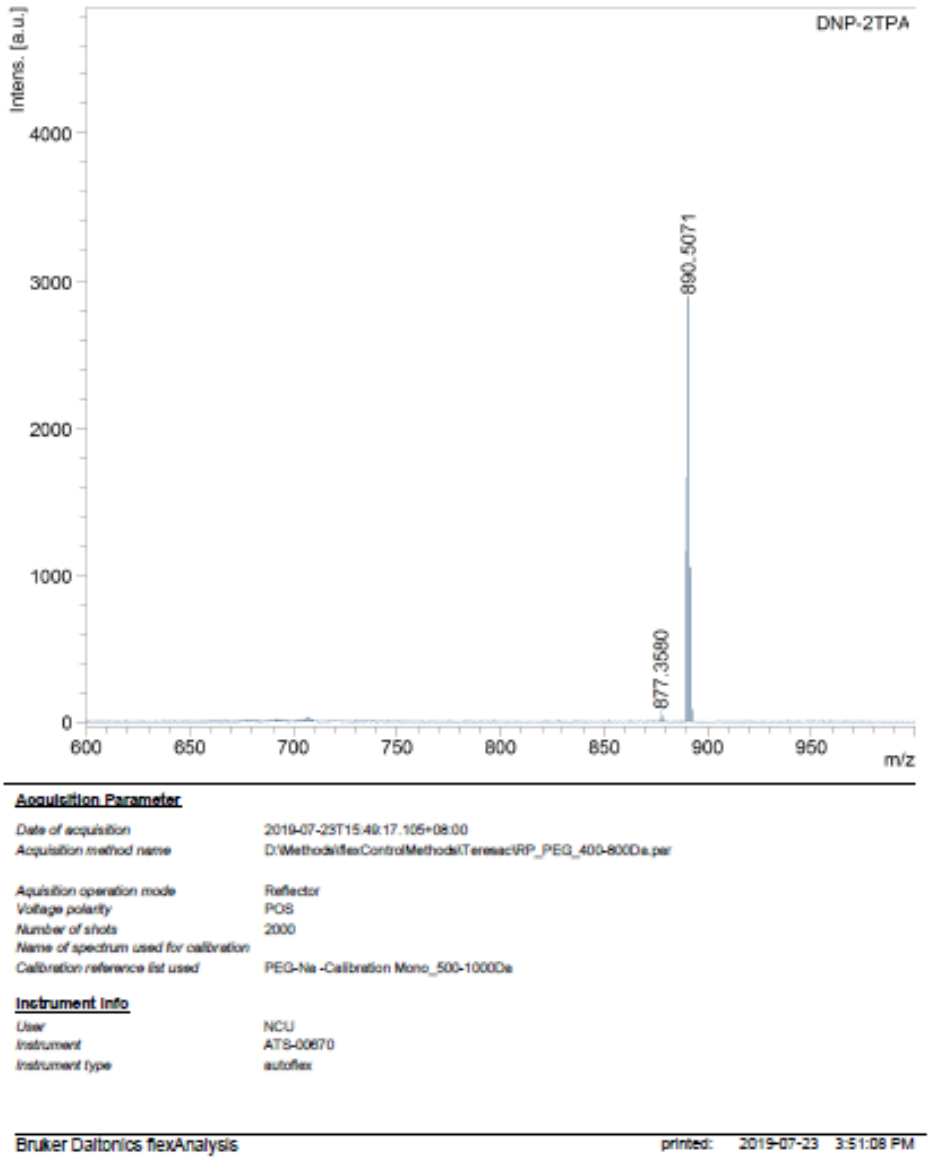

2.3. Mass Spectra of bDNB (Exact Mass = 1774.7195)

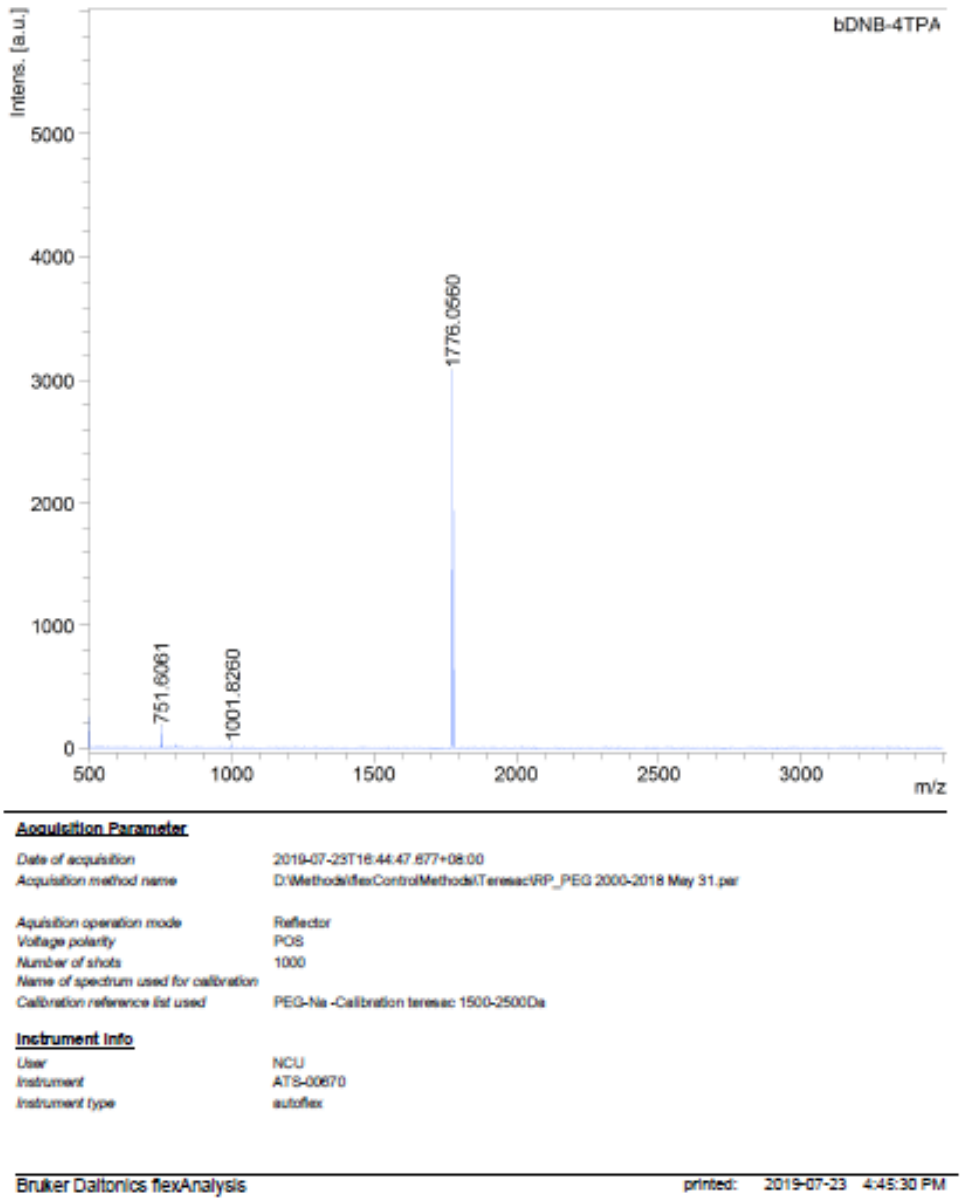

3. Optical, Thermal and Electrochemical Properties of Final Compounds

Compound	TGA (°C)[a]	UV-Vis λ_{max}[b] (nm)	E_{gap} (eV)		DPV(eV)[e]			
			DPV[c]	UV-Vis[d]	E_{re} (V)	E_{ox} (V)	HOMO	LUMO
DNB	437.3	348	2.57	2.65	-1.74	0.83	-5.03	-2.46
bDNB	445.6	356	2.26	2.50	-1.44	0.82	-5.02	-2.76
DNP	400.9	350	2.10	2.49	-1.33	0.78	-4.98	-2.87

[a] 5%weight loss, measured by TGA.

[b] use *o*-dichlorobenzene as a solvent.

[c] E_{gap} = LUMO-HOMO.

[d] calculated based on λ_{onset}, E_{gap} = 1240/ λ_{onset}.

[e] all potential reported by DPV with ferrocene as internal standard in *o*-dichlorobenzene, LUMO = -(E_{re} + 4.2), HOMO = -(E_{ox} + 4.2)